# Molecular Spectroscopy beyond the Born−Oppenheimer Approximation: A Computational Study of the $CF_3O$ and $CF_3S$ Radicals†

**Aleksandr V. Marenich and James E. Boggs***

*Institute for Theoretical Chemistry, Department of Chemistry and Biochemistry, The University of Texas at Austin, 1 University Station A5300, Austin, Texas 78712−0165*

*Received: January 19, 2007; In Final Form: February 20, 2007*

This paper addresses some advances in the theoretical description of molecular spectroscopy beyond the Born−Oppenheimer adiabatic approximation. A solution of the nuclear dynamics problem complicated by the E⊗E Jahn−Teller effect and spin−orbit coupling is considered for the case of the $CF_3O$ and $CF_3S$ radicals, all the model parameters being obtained solely from ab initio calculations without any adjustment to experimental numbers. Vibrational and vibronic model parameters were calculated at the equation-of-motion coupled cluster level of theory with basis sets of triple-$\zeta$ quality. The spin−orbit coupling in $\tilde{X}\ ^2E$ $CF_3O$ and $CF_3S$ was parametrized by means of a perturbative solution of the full Breit−Pauli spin−orbit operator. Spin-vibronic eigenvalues and eigenfunctions were computed in a basis set of products of electronic, electron spin, and vibrational functions. Results demonstrate the importance of explicit inclusion of the spin−orbit coupling and at least cubic Jahn−Teller terms in the model Hamiltonian for the high precision evaluation of spin-vibronic energy levels of $CF_3O$ and $CF_3S$. The theoretical results support and complement the spectroscopic data observed for these species.

## Introduction

The Born−Oppenheimer approximation[1] has been one of the cornerstones of modern molecular and chemical physics, and it will remain such in many cases when an approximate separation of the nuclear and electronic motion can be valid. However, a recent review[2] has indicated the growth of interest from both theoreticians and experimentalists in studying nonadiabatic dynamics and its manifestation in molecular spectroscopy when the nuclear motion is ruled by two or more potential energy surfaces corresponding to vibronically coupled electronic states. High-resolution experimental techniques (such as femtosecond real-time spectroscopy,[3] laser-induced spectroscopy coupled with supersonic free jet cooling,[4,5] rotationally resolved stimulated emission pumping,[6] etc.) have been elaborated to reveal more spectral features and to produce more information about nuclear dynamics. On the other hand, the accuracy of modern theoretical methods has increased significantly due to the development of advanced techniques in electronic structure theory and the growth of computational capacities. Hence, this joint progress of experiment and first-principle theory stimulates a new interest in the study of nonadiabatic effects, which may have a significant impact on the spectroscopic and structural properties of a large variety of molecules and radicals.

A breakdown of the Born−Oppenheimer adiabatic approximation is expected in the case of close-lying electronic states and conical intersections due to a nonvanishing derivative coupling $F_{ij} = \langle \Psi_i | \nabla_Q \Psi_j \rangle$ between two adiabatic electronic states $\Psi_i$ and $\Psi_j$, where the gradient $\nabla_Q$ is a vector in the nuclear coordinate ($Q$) space.[2] Approaching the conical intersection of the corresponding adiabatic potential energy surfaces, the derivative coupling $F_{ij}$ becomes singular, giving rise to a vibrational-electronic (*vibronic*) interaction so that the traditional Born−Oppenheimer approximation becomes meaningless. In this case, the nuclear dynamics problem must be solved for a manifold of coupled electronic states assumed to be well-separated from the others. Nonadiabatic derivative coupling terms can be negligibly small upon the unitary transformation of an adiabatic basis set to a new basis called diabatic[2,7] (or approximately diabatic for a general case of polyatomic molecules, see the discussion in ref 8). The kinetic part of the nuclear Hamiltonian becomes diagonal. In contrast, the potential energy matrix constructed in terms of diabatic electronic states contains off-diagonal elements responsible for the coupling between electronic states.[2] The problems related to the adiabatic states such as the geometry dependent (Berry) phase[9] that is acquired by an adiabatic electronic wavefunction transposed around the intersection[10,11] (see also a recent analysis[12] of the Berry phase for the ozone molecule) can be avoided using the concept of diabatic electronic states that are single-valued because the corresponding derivative coupling should vanish.

We consider a case of symmetry-required conical intersections[13] induced by the Jahn−Teller (JT) effect[14] as the source of the structural instability of high-symmetry nuclear configurations of polyatomic systems.[15,16] The nuclear dynamics for the 2-fold degenerate electronic term can be described beyond the Born−Oppenheimer approximation by means of the 2 × 2 diabatic potential energy matrix[2,16]

$$\begin{pmatrix} V_{11} & V_{12} \\ V_{21} & V_{22} \end{pmatrix} = \begin{pmatrix} A+B & C \\ C & A-B \end{pmatrix} \qquad (1)$$

Functions $B$ and $C$ refer to the JT vibronic coupling between two components of the degenerate electronic state. Element $A$ is a so-called unperturbed potential surface[2] that contains no vibronic coupling but may include anharmonic effects. Because the JT adiabatic potentials $\epsilon_\pm = A \pm \sqrt{C^2+B^2}$ are eigenvalues

† Part of the "Thom H. Dunning, Jr., Festschrift".

* To whom correspondence should be addressed. E-mail: james.boggs@mail.utexas.edu.

10.1021/jp070495f CCC: $37.00 
Published on Web 05/01/2007

of eq 1, the diabatic matrix in our case can be constructed solely from the two adiabatic surfaces $\epsilon_\pm$ that can be calculated routinely using an appropriate quantum chemistry method; knowledge of the adiabatic electronic wavefunctions is not required. Due to symmetry restrictions it is sufficient to determine $A$ and $B$ in eq 1, the $C$ element is expressed via $B$. The adiabatic potential energy surfaces $\epsilon_\pm = A \pm \sqrt{C^2+B^2}$, fragments of which are depicted in Figure 1a, contain the singularity at the point of conical intersection while the elements of the diabatic potential energy matrix $V_{11}$, $V_{22}$, $V_{12}$ in eq 1 are smooth functions of nuclear coordinates. The diabatic potential energy surfaces $V_{11}$ and $V_{22}$ in Figure 1b still intersect but in the one-dimensional subspace (there is no conical intersection).

The vibronic matrix elements in eq 1 can be approximated as Taylor series in the nuclear coordinate space at the point of conical intersection. The linear Jahn−Teller terms dominate in this expansion because the electronic degeneracy is lifted in a linear way at the vicinity of conical intersection (Figure 1a), giving rise to the well-know "Mexican hat" adiabatic potential surface.[16] The Taylor expansion of the vibronic terms $B$ and $C$ in eq 1 is usually truncated at the second-order coupling (see references in ref 16), which may not be quite enough for the most accurate description of the JT dynamics. The authors of ref 17 showed the importance of extension of the model Hamiltonian of $^2E'$ $NO_3$ beyond the linear and quadratic JT couplings using vibronic parameters of up to the sixth order. There is a distinct lack of theoretical calculations with inclusion of JT terms of higher than second order. The JT Hamiltonians for different vibrational modes do not commute and cannot be treated separately. Therefore, the multimode vibronic coupling cannot be neglected in polyatomic molecules.[2] Anharmonic effects, mostly ignored in JT calculations, should also be included, as they may be responsible for the warping of the JT potential energy surfaces[18] that can affect the vibronic dynamics. Finally, the spin−orbit coupling (if it is not small) should be explicitly introduced into the model Hamiltonian. The role of spin−orbit coupling (SOC) in quenching the Jahn−Teller effect and vice versa has been discussed in the literature.[4,19,20]

In this paper we report the results of a computational study of the nuclear dynamics in the ground electronic state $\tilde{X}$ $^2E$ of the $CF_3O$ and $CF_3S$ radicals that are fluorinated analogs of the methoxy radical $CH_3O$. An accurate prediction of molecular properties of the methoxy family radicals $CL_3X$ (ligand $L$ = H, F; $X$ = O, S) as important intermediates in environmental chemistry is critical for practical applications. The $CF_3O$ and $CF_3S$ radicals have been studied experimentally and theoretically (see refs 20 and 21 and therein).

## Computational Details

**Spin-Vibronic Model.** There are six normal vibrations ($Q$) determined for the $C_{3v}$ symmetry nuclear configuration of $CF_3X$ ($X$ = O, S): symmetric C$X$ stretching $Q_1(A_1)$, $CF_3$ stretching $Q_2(A_1)$, $CF_3$ deformation $Q_3(A_1)$, asymmetric $CF_3$ stretching $Q_4(E)$, FCF deformation (scissors) $Q_5(E)$, and FC$X$ deformation $Q_6(E)$. As predicted by the Jahn−Teller theorem,[14] the ground electronic state $\tilde{X}$ $^2E$, possessing a molecular orbital of E symmetry occupied by an unpaired electron, in the absence of spin−orbit coupling is expected to be unstable ($E \rightarrow A' + A''$) with respect to distortion of the equilibrium nuclear configuration along the asymmetric (JT active) vibrational modes with appearance of a conical intersection at the $C_{3v}$ symmetry point and three equivalent minima of $C_s$ symmetry on the low branch of the potential energy surface.

The nonzero spin−orbit coupling in the methoxy family species can significantly reduce the JT effect.[4,20] According to our previous computations,[21−23] the JT distortions in the sulfur-centered species ($CH_3S$ and $CF_3S$) are totally quenched by the strong SOC, meaning that the $C_{3v}$ symmetry of the equilibrium nuclear configuration is preserved. On the other hand, the $CH_3O$ and $CF_3O$ radicals are structurally distorted by the JT effect accompanied by a relatively small SOC. This conclusion is in agreement with results of the earlier laser-induced spectroscopy study of these species.[4,20]

Our analysis[21−23] of the Jahn−Teller effect in $\tilde{X}$ $^2E$ $CL_3X$ indicates that these species are strongly nonadiabatic systems that require a treatment beyond the Born−Oppenheimer approximation by means of a variational solution of the nuclear Schrödinger equation for two strongly coupled electronic states correlating to the 2-fold degenerate electronic state at the $C_{3v}$ symmetry nuclear configuration. The interplay of Jahn−Teller and spin−orbit couplings in $\tilde{X}^2E$ $CL_3X$ gives rise to spin-vibronic interactions so that neither of these effects can be neglected; they must be treated on an equal footing. In the absence of external magnetic fields the total Hamiltonian commutes with the time-reversal operator so that at least the 2-fold degeneracy (Kramers degeneracy) with respect to spin is expected for a system with an odd number of electrons in addition to the spatial degeneracy.[24] The spinless matrix in eq 1 should be modified accordingly to account for the vibronic coupling between two Kramers doublets.

The approximate spin-vibronic model Hamiltonian describing the dynamics of electrons and nuclei in the ground electronic state $\tilde{X}$ $^2E$ of $CF_3O$ and $CF_3S$ is obtained in terms of four complex-valued diabatic spin-orbitals $\Phi_i$ with the use of findings in refs 4, 20 25−27 (see also details of our previous dynamics studies[22,23] of the $CH_3O$ and $CH_3S$ radicals):

$$\begin{pmatrix} \left(\hat{T}+V_0-\frac{1}{2}a\zeta_e\right)-E & V_{-+} & 0 & 0 \\ V_{+-} & \left(\hat{T}+V_0+\frac{1}{2}a\zeta_e\right)-E & 0 & 0 \\ 0 & 0 & \left(\hat{T}+V_0+\frac{1}{2}a\zeta_e\right)-E & V_{-+} \\ 0 & 0 & V_{+-} & \left(\hat{T}+V_0-\frac{1}{2}a\zeta_e\right)-E \end{pmatrix} \begin{pmatrix} \chi(\Phi_1) \\ \chi(\Phi_2) \\ \chi(\Phi_3) \\ \chi(\Phi_4) \end{pmatrix} = 0 \qquad (2)$$

where complex-valued nuclear basis functions $\chi$ are constructed for each electronic state $\Phi_i$ as products of one-dimensional and two-dimensional isotropic harmonic oscillator eigenstates; $\hat{T}$ is the nuclear kinetic energy operator; matrix elements of the electronic Hamiltonian $V_0 = \langle\Phi_i|\hat{H}_e|\Phi_i\rangle$ and $V_{+-} = (V_{-+})^* = \langle\Phi_{2,4}|\hat{H}_e|\Phi_{1,3}\rangle$ are spinless vibrational and vibronic potential energy functions,

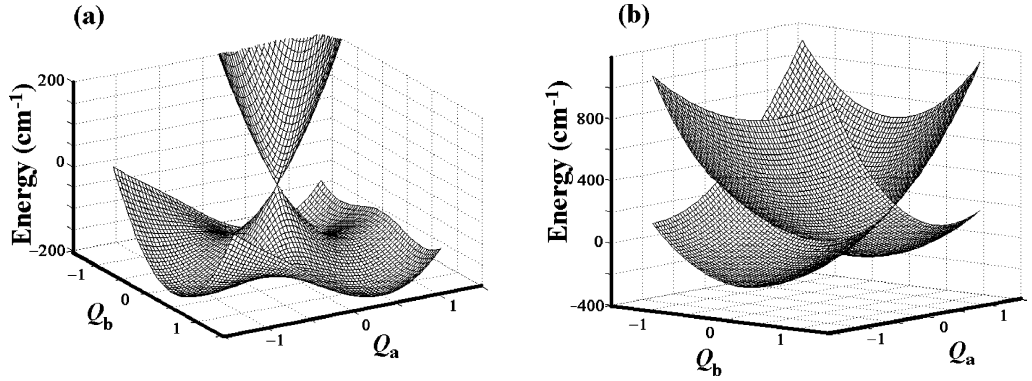


**Figure 1.** Fragments of (a) the adiabatic potential energy surfaces and (b) diagonal elements of the diabatic potential energy matrix for $\tilde{X}$ $^2E$ $CF_3O$ in the vicinity of a conical intersection where $Q_a$ and $Q_b$ are dimensionless real components of the degenerate FCO-deformation normal mode.

**TABLE 1: Nonzero Matrix Elements of Operators $Q_{\pm}^n$ ($n = 0-4$) and $Q_+^m Q_-^n$ ($m, n = 1$ or 2)[a]**

$\langle v, l|v, l\rangle = 1$
$\langle v \pm 1, l + 1|Q_+|v, l\rangle = [(v \pm l + 1 \pm 1)/2\gamma]^{1/2}$
$\langle v \pm 1, l - 1|Q_-|v, l\rangle = [(v \mp l + 1 \pm 1)/2\gamma]^{1/2}$
$\langle v, l \pm 2|Q_\pm^2|v, l\rangle = [(v \pm l + 2)(v \mp l)]^{1/2}/\gamma$
$\langle v \pm 2, l + 2|Q_+^2|v, l\rangle = [(v \pm l \pm 2)(v \pm l + 2 \pm 2)]^{1/2}/2\gamma$
$\langle v \pm 2, l - 2|Q_-^2|v, l\rangle = [(v \mp l \pm 2)(v \mp l + 2 \pm 2)]^{1/2}/2\gamma$
$\langle v, l|Q_+Q_-|v, l\rangle = (v + l)/\gamma$
$\langle v \pm 2, l|Q_+Q_-|v, l\rangle = [(v + l + 1 \pm 1)(v - l + 1 \pm 1)]^{1/2}/2\gamma$
$\langle v \pm 3, l + 3|Q_+^3|v, l\rangle = [(v \pm l + 3 \pm 3)(v \pm l \pm 2)(v \pm l \pm 4)(2\gamma)^{-3}]^{1/2}$
$\langle v \pm 3, l - 3|Q_-^3|v, l\rangle = [(v \mp l + 3 \pm 3)(v \mp l \pm 2)(v \mp l \pm 4)(2\gamma)^{-3}]^{1/2}$
$\langle v \pm 1, l + 3|Q_+^3|v, l\rangle = 3[(v - l)(v \pm l \pm 2)(v + l + 3 \pm 1)(2\gamma)^{-3}]^{1/2}$
$\langle v \pm 1, l - 3|Q_-^3|v, l\rangle = 3[(v + l)(v \mp l \pm 2)(v - l + 3 \pm 1)(2\gamma)^{-3}]^{1/2}$
$\langle v \pm 3, l + 1|Q_+^2Q_-|v, l\rangle = [(v \pm l \pm 2)(v - l + 1 \pm 1)(v + l + 2 \pm 2)(2\gamma)^{-3}]^{1/2}$
$\langle v \pm 3, l - 1|Q_+Q_-^2|v, l\rangle = [(v \mp l \pm 2)(v + l + 1 \pm 1)(v - l + 2 \pm 2)(2\gamma)^{-3}]^{1/2}$
$\langle v \pm 1, l + 1|Q_+^2Q_-|v, l\rangle = (3v \mp l + 3 \pm 1)\,[(v \pm l + 1 \pm 1)(2\gamma)^{-3}]^{1/2}$
$\langle v \pm 1, l - 1|Q_+Q_-^2|v, l\rangle = (3v \pm l + 3 \pm 1)\,[(v \mp l + 1 \pm 1)(2\gamma)^{-3}]^{1/2}$
$\langle v \pm 4, l + 4|Q_+^4|v, l\rangle = [(v \pm l \pm 6)(v \pm l \pm 6 + 2)(v \pm l \pm 2)(v \pm l \pm 2 + 2)]^{1/2}/(2\gamma)^2$
$\langle v \pm 4, l - 4|Q_-^4|v, l\rangle = [(v \mp l \pm 6)(v \mp l \pm 6 + 2)(v \mp l \pm 2)(v \mp l \pm 2 + 2)]^{1/2}/(2\gamma)^2$
$\langle v \pm 2, l + 4|Q_+^4|v, l\rangle = [(v \pm l \pm 4)(v \pm l \pm 4 + 2)(v + l + 2)(v - l)]^{1/2}/2\gamma^2$
$\langle v \pm 2, l - 4|Q_-^4|v, l\rangle = [(v \mp l \pm 4)(v \mp l \pm 4 + 2)(v - l + 2)(v + l)]^{1/2}/2\gamma^2$
$\langle v, l \pm 4|Q_\pm^4|v, l\rangle = 3[(v \pm l + 4)(v \pm l + 2)(v \mp l)(v \mp l - 2)]^{1/2}/2\gamma^2$
$\langle v \pm 4, l|(Q_+Q_-)^2|v, l\rangle = [(v + l + 2 \pm 2)(v - l + 2 \pm 2)(v + l \pm 2)(v - l \pm 2)]^{1/2}/(2\gamma)^2$
$\langle v \pm 2, l|(Q_+Q_-)^2|v, l\rangle = (v + 1 \pm 1)\,[(v + l + 1 \pm 1)(v - l + 1 \pm 1)]^{1/2}/\gamma^2$
$\langle v, l|(Q+Q_-)^2|v, l\rangle = (3v^2 + 6v + 4 - l^2)/2\gamma^2$

[a] The value of $\gamma$ is set to $\gamma = 1$ if a normal coordinate $Q$ is dimensionless, and $\gamma = \omega\ [m_e^{-1}a_o^{-2}]$ if $Q$ is a mass-weighted coordinate expressed in Hartree units, where $\omega$ is the corresponding harmonic oscillator frequency.

respectively; and the value of $a\zeta_e = 2|\pm\langle\Phi_i|\hat{H}_{SO}|\Phi_i\rangle|$ (where $\hat{H}_{SO}$ is a spin−orbit operator) refers to the magnitude of the spin−orbit splitting in $\tilde{X}$ $^2E$ $CF_3O$ and $CF_3S$. The electronic basis states ($\Phi_1$, $\Phi_4$) and ($\Phi_2$, $\Phi_3$) are two Kramers doublets transformed in accordance with the double $C_{3v}$ symmetry group[28−30] representations $E_{3/2}$ and $E_{1/2}$, respectively. The nuclear problem can be solved for just one of the blocks in eq 2 distinguished only upon time reversal.

For the sake of simplicity, we can assume that the spin−orbit operator $\hat{H}_{SO}$ does not depend on the nuclear coordinates at least in the vicinity of the conical intersection and it can be treated in the phenomenological manner as $\hat{H}_{SO} = a\hat{L}\hat{S}$ using the molecule-fixed axis projections of the electronic orbital $\hat{L}_\alpha$ and electronic spin $\hat{S}_\alpha$ momenta ($\alpha = x, y, z$) and excluding the spin−orbit coupling between the states of different $L$ and $S$, the $a$ quantity being a constant. The electronic basis set $\Phi_i$ can be expressed in terms of products of spatial electronic wavefunctions $|\Lambda\rangle$ and spin electronic states $|S, m_s\rangle$ as $\Phi_1 = |-1\rangle|1/2, -1/2\rangle$, $\Phi_2 = |+1\rangle|1/2, -1/2\rangle$, $\Phi_3 = |-1\rangle|1/2, +1/2\rangle$, and $\Phi_4 = |+1\rangle|1/2, +1/2\rangle$, where the value of $\Lambda = \pm 1$ distinguishes two complex components of the degenerate electronic state. According to the literature,[4,28] the phenomenological spin−orbit operator $\hat{H}_{SO} = a\hat{L}\hat{S}$ is diagonal in the basis of $\Phi_i$ due to the $C_{3v}$ symmetry of the molecules of interest and the time-reversal properties of functions $\Phi_i$: only elements $\langle\Lambda|a\hat{L}_z|\Lambda\rangle\langle m_s|\hat{S}_z|m_s\rangle = -a\zeta_e\Lambda m_s$ are nonvanishing.[28] Thus, in terms of the model presented above we can describe the spin−orbit coupling in $\tilde{X}$ $^2E$ $CL_3X$ by using a single parameter $a\zeta_e$ equal to the value of spin−orbit splitting in the $\tilde{X}$ $^2E$ electronic state at the point of the conical intersection corresponding to the $C_{3v}$ symmetry nuclear configuration. A value of $a\zeta_e$ can be derived from spectroscopic data[4] or can be calculated ab initio. We calculate the value of $a\zeta_e$ using the microscopic (Breit−Pauli) spin−orbit operator (see details below). Applying this approximation, we should clarify that, unlike the simplified model of $\hat{H}_{SO} = a\hat{L}_z\hat{S}_z$ used to define a spin−orbit operator in the present study, the Breit−Pauli operator as shown in ref 31 (in the one-electron approximation) may not be strictly diagonal in terms of the electronic basis functions $\Phi_i$ introduced in eq 2, and it becomes diagonal in the new diabatic basis obtained as a linear combination of $\Phi_i$.[31]

The electronic potential matrix elements $V_0$ and $V_{+-} = (V_{-+})^*$ are expressed through symmetry-adapted Taylor series

using the complex $Q_{\pm} = Q_a \pm iQ_b$ components of 2-fold degenerate normal modes $Q$(E):

$$V_0 = \sum_{i=1}^{3}\frac{1}{2!}\omega_i Q_i^2 + \sum_{i=4}^{6}\frac{1}{2!}\omega_i Q_{i+}Q_{j-} + \sum_{i=1}^{3}\frac{1}{3!}f_{iii}Q_i^3 + \sum_{i=4}^{6}\frac{1}{3!2}f_{iii}(Q_{i+}^3 + Q_{i-}^3) + \frac{1}{2!2}f_{556}(Q_{5+}^2Q_{6+} + Q_{5-}^2Q_{6-}) + \frac{1}{2!2}f_{566}(Q_{5+}Q_{6+}^2 + Q_{5-}Q_{6-}^2) + \sum_{i=1}^{3}\frac{1}{4!}f_{iiii}Q_i^4 + \sum_{i=4}^{6}\frac{1}{4!}f_{iiii}Q_{i+}^2Q_{i-}^2 + \frac{1}{2!2!}f_{5566}Q_{5+}Q_{5-}Q_{6+}Q_{6-} \quad (3)$$

where the vibrational potential function $V_0$ contains not only a harmonic part including the $\omega_i$ quantities equal to diabatic harmonic frequencies calculated for the three nondegenerate and three 2-fold degenerate vibrational modes but also anharmonic contributions from cubic ($f_{iii}$) and quartic ($f_{iiii}$) terms including the intermode coupling ($f_{556}$, $f_{566}$, $f_{5566}$) between the two deformations $Q_5$(E) and $Q_6$(E) that generate the most pronounced net JT effects in $\tilde{X}\ ^2$E $CF_3O$ and $CF_3S$.[21] The vibronic parts $V_{+-}$ and $V_{-+}$ are expressed through linear ($k_4$, $k_5$, $k_6$), quadratic ($g_{44}$, $g_{55}$, $g_{66}$, $g_{56}$), cubic ($g_{444}$, $g_{555}$, $g_{666}$, $g_{556}$, $g_{566}$), and quartic JT ($g_{4444}$, $g_{5555}$, $g_{6666}$, $g_{5566}$) constants as follows:

$$V_{\pm\mp} = \sum_{i=4}^{6}k_iQ_{i\mp} + \sum_{i=4}^{6}\frac{1}{2!}g_{ii}Q_{i\pm}^2 + g_{56}Q_{5\pm}Q_6\pm + \sum_{i=4}^{6}\frac{1}{3!}g_{iii}Q_{i\pm}Q_{i\mp}^2 + \frac{1}{2!}g_{556}Q_{5\pm}Q_{5\mp}Q_{6\mp} + \frac{1}{2!}g_{566}Q_{5\mp}Q_{6\pm}Q_{6\mp} + \sum_{i=4}^{6}\frac{1}{4!}g_{iiii}Q_{i\mp}^4 + \frac{1}{2!2!}g_{5566}Q_{5\mp}^2Q_{6\mp}^2 \quad (4)$$

The spin-vibronic E⊗E eigenproblem of eq 2 was solved using the orthonormalized harmonic oscillator eigenfunctions expressed via Hermite polynomials[29] including all the $CF_3X$ ($X$ = O, S) normal coordinates $Q$. Table 1 shows nonzero matrix elements of operators $Q_{i\pm}^n$ ($n = 0 - 4$) and $Q_{i+}^mQ_{i-}^n$ ($m$, $n$ = 1 or 2) used for a solution of eq 2 in terms of wavefunctions $|v_i, l_i\rangle$ of the two-dimensional isotropic harmonic oscillator, where the integers $v_i$ and $l_i$ refer to the principal vibrational and vibrational angular momentum quantum numbers, respectively ($l_i = v_i, v_i - 2, v_i - 4, ...$).[29] Our tests show that the variational limit at least for those spin-vibronic levels that correspond to the fundamental vibrational transitions in $\tilde{X}\ ^2$E $CF_3O$ and $CF_3S$ can be achieved with values of $v_i$ not larger than 5. Each spin-vibronic basis function is a product of the spin−orbit electronic wave function $\Phi_i$ characterized by a quantum number of the total electronic momentum $\vec{J} = \vec{L} + \vec{S}$ ($m_J = \pm 1/2, \pm 3/2$) and the vibrational part described in terms of the total vibrational angular momentum $l$. The symmetry of spin-vibronic states is defined as $E_{3/2}$ if the value of $2|m_J + l|$ is a multiple of 3 or as $E_{1/2}$ if it is not. On the other hand, vibronic levels (if no SOC included) can be classified according to the symmetry of E⊗E = $A_1 + A_2 + E$ and the Jahn−Teller quantum number $j_{JT} = l + 1/2\Lambda$. The latter may not be a good number if nonlinear terms are included in the JT Hamiltonian but can be useful for an approximate interpretation.

The nonadiabatic (pseudo-Jahn−Teller) coupling of the ground $\tilde{X}\ ^2$E and first excited $\tilde{A}\ ^2A_1$ electronic states was found small in the case of $CH_3S$;[23] therefore, we can safely neglect this effect in the spin-vibronic Hamiltonian of $CF_3O$ and $CF_3S$, the fluorinated analogs of $CH_3S$.

**TABLE 2: Molecular Properties ($cm^{-1}$) of $\tilde{X}\ ^2$E $CF_3O$ and $CF_3S$[a]**

| | vibrational parameters | | | vibronic parameters | |
|---|---|---|---|---|---|
| | $CF_3O$ | $CF_3S$ | | $CF_3O$ | $CF_3S$ |
| $\omega_1(A_1)$ | 1332 (C−O) | 796 (C−S) | $E_{JT}$ | 224 | 81 |
| $\omega_2(A_1)$ | 939 (C−F) | 1189 (C−F) | $\Delta_{JT}$ | 40 | 15 |
| $\omega_3(A_1)$ | 646 ($CF_3$) | 471 ($CF_3$) | $a\zeta_e$ | 133 | 387 |
| $\omega_4$(E) | 1320 (C−F) | 1253 (C−F) | $a\zeta_e d$ | 42 | 165 |
| $\omega_5$(E) | 621 (FCF) | 561 (FCF) | | | |
| $\omega_6$(E) | 433 (FCO) | 322 (FCS) | $k_4$ | −31 | −17 |
| $f_{111}$ | 207 | 110 | $k_5$ | −153 | −20 |
| $f_{222}$ | −136 | −47 | $k_6$ | −393 | −215 |
| $f_{333}$ | 22 | −59 | $g_{44}$ | 35 | 18 |
| $f_{444}$ | 236 | 234 | $g_{55}$ | 56 | 13 |
| $f_{555}$ | 56 | −68 | $g_{66}$ | 30 | 42 |
| $f_{666}$ | −49 | −37 | $g_{444}$ | −7 | −3 |
| $f_{1111}$ | 67 | 16 | $g_{555}$ | −5 | 1.6 |
| $f_{2222}$ | 16 | 14 | $g_{666}$ | −8 | −6 |
| $f_{3333}$ | 19 | −14 | $g_{4444}$ | 1.4 | 1.2 |
| $f_{4444}$ | 107 | 105 | $g_{5555}$ | 0.8 | −0.4 |
| $f_{5555}$ | 21 | 29 | $g_{6666}$ | 0.05 | 3 |
| $f_{6666}$ | 8 | 10 | $g_{56}$ | 47 | −28 |
| $f_{566}$ | −7 | −13 | $g_{556}$ | −3 | −0.7 |
| $f_{556}$ | −18 | 10 | $g_{566}$ | −5 | 1.2 |
| $f_{5566}$ | 8 | −0.3 | $g_{5566}$ | 1.1 | 0.3 |

[a] Jahn−Teller stabilization energies ($E_{JT}$) and barriers to pseudorotation ($\Delta_{JT}$), values of spin−orbit splitting ($a\zeta_e$), and harmonic frequencies ($\omega$) are taken from our previous study[21] of $CF_3O$ and $CF_3S$. A value of $a\zeta_e d$ indicates the magnitude of spin−orbit splitting in the zero vibronic state $0_0$(E). See eqs 3 and 4 for definition of other quantities.

**Electronic Structure Calculation.** In the present paper, vibrational and vibronic parameters in eqs 3 and 4 have been found by numerical differentiation of eqs 3 and 4 using the least-square fitting of model adiabatic potential energy surfaces to single point energies calculated ab initio over 136 nuclear configurations distorted in the vicinity of the conical intersection corresponding to the $C_{3v}$ symmetry configuration optimized in our previous study;[21] see also ref 23 for more details. The distorted nuclear configurations were generated using symmetry-adapted vibrational coordinates **S** related to the normal coordinates as $\mathbf{S} = \mathbf{LQ}$. The harmonic analysis of the $C_{3v}$ symmetry configuration was performed using the program ANOCOR.[32] Ab initio adiabatic single point energies of the two electronic states arising from $\tilde{X}\ ^2$E were calculated with a local version of the ACES II program package[33] employing the equation-of-motion method[34,35] with the coupled cluster singles and doubles (CCSD) reference wavefunction for the $CF_3X^-$ anion ground state (further abbreviated as EOMIP-CCSD or EOMIP). We used the correlation consistent polarized valence basis sets[36] of Dunning et al. of triple-$\zeta$ quality including extra functions[37] for C, F, O, and S to account for core−core and core−valence correlation (cc-pCVTZ).[38] The linear combinations of symmetry-adapted basis functions used only pure spherical harmonics. The total number of basis functions included in the molecular orbital (MO) variation spaces was 215 ($CF_3O$) and 231 ($CF_3S$). No core MOs were dropped in coupled cluster calculations of $CF_3X$.

The value of $a\zeta_e = 133$ ($CF_3O$) and 387 ($CF_3S$) $cm^{-1}$ used in eq 2 was calculated in our previous study[21] as a magnitude of the spin−orbit splitting of $\tilde{X}\ ^2$E at the point of conical intersection corresponding to the $C_{3v}$ symmetry configuration optimized at the EOMIP/cc-pCVTZ level of theory. The calculation of $a\zeta_e$ was carried out by the GAMESS program[39] as a perturbative solution of the full (one-electron $1\bar{e}$ and two-electron $2\bar{e}$) Breit−Pauli spin−orbit operator[40] using multicon-

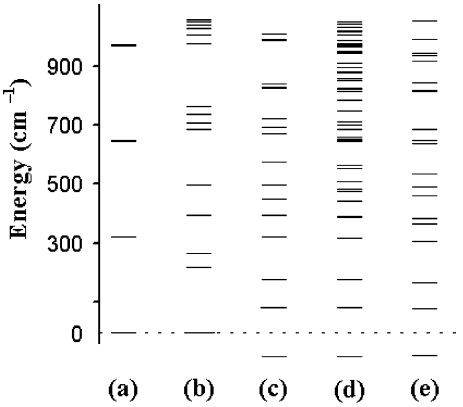


**Figure 2.** Eigenstates of eq 2 for $\tilde{X}$ $^2$E $CF_3S$ calculated (a) in the single mode ($Q_6$) approximation without inclusion of any spin-vibronic effects and (b) with inclusion of the JT effect, (c) with inclusion of the JT effect and SOC. (d) Spin-vibronic eigenstates calculated with inclusion of all vibrational modes. (e) Experimental wavenumbers observed in the laser-induced dispersed fluorescence spectrum of $CF_3S$.[20] All energies are related to the corresponding ground state (a), (b) or to the middle of the spin−orbit splitting in the ground vibronic state (c)−(e).

figuration quasi-degenerate second-order perturbation theory[41] based on a state-averaged complete active space CASSCF wavefunction with the cc-pCVTZ basis set. We also included 1$\bar{e}$ and 2$\bar{e}$ scalar relativistic corrections to the SOC integrals by means of elimination of the small components of relativistic wavefunctions (the RESC scheme).[42] The CAS consisted of five electrons in four orbitals ($2A_1 + E$) where the E orbitals could be interpreted as the O 2p$\pi$ or S 3p$\pi$ lone pairs and the $A_1$ orbitals as the C−O or C−S $\sigma$ and $\sigma$* MOs. The theoretical values of $a\zeta_e$ = 133 ($CF_3O$) and 387 ($CF_3S$) cm$^{-1}$ are very close to the corresponding experimental values, 140 ($CF_3O$) and 360 ($CF_3S$) cm$^{-1}$, derived from the fluorescence spectra of these radicals.[20]

## Results and Discussion

Table 2 shows values of vibronic and force constants calculated for the ground electronic state $\tilde{X}$ $^2$E of $CF_3O$ and $CF_3S$. Force constants ($f$) in $\tilde{X}$ $^2$E $CF_3O$ and $CF_3S$ are relatively small, indicating smaller anharmonic effects than those in $\tilde{X}$ $^2$E $CH_3O$ and $CH_3S$.[22,23] For instance, the absolute values of the cubic force constants corresponding to the C−H stretching in $CH_3O$ and $CH_3S$ vary from 808 to 1131 cm$^{-1}$ (refs 22 and 23), whereas the values of $f$(C−F) vary in the range 47−236 cm$^{-1}$. Force constants ($f_{555}$, $f_{666}$, $f_{566}$, $f_{556}$) corresponding to the Jahn−Teller active modes $Q_5$(E) and $Q_6$(E) are even smaller, but they are comparable in value with the corresponding vibronic constants ($g_{55}$, $g_{66}$, $g_{56}$) and they, along with quadratic JT coupling, may be responsible for an additional warping[18] of the JT potential energy surfaces. Our calculation shows that the inclusion of $f_{555}$, $f_{666}$, $f_{566}$, and $f_{556}$ in the model Hamiltonian as indicated in eq 3 provides a noticeable shift of the spin-vibronic energy levels related to $Q_5$(E) and $Q_6$(E) (by ∼50 cm$^{-1}$).

Analysis of the values of vibronic constants shows that the most prominent net Jahn−Teller effect is observed along the FC$X$ deformation $Q_6$(E). A vibronic coupling ($g_{56}$) between $Q_5$-(E) and $Q_6$(E) is quite significant (28−47 cm$^{-1}$) in comparison with $g_{55}$ and $g_{66}$ and cannot be neglected. The role of higher order Jahn−Teller terms (cubic and quartic) in the model Hamiltonian was clarified by comparison of vibronic energy levels calculated with inclusion of only linear and quadratic JT terms, then with inclusion of linear, quadratic, and cubic terms, and finally, with all of the terms in eq 4 including the quartic JT coupling. This analysis indicates that the spin-vibronic dynamics in $\tilde{X}$ $^2$E $CF_3S$ can be well described using only linear and quadratic JT terms in eq 4, whereas the inclusion of higher order terms for $\tilde{X}$ $^2$E $CF_3O$ is more vital for a better accuracy as the Jahn−Teller effect in $\tilde{X}$ $^2$E $CF_3O$ is stronger than in $\tilde{X}$ $^2$E $CF_3S$ (cf. the JT stabilization energies and linear JT constants in Table 2).

**TABLE 3: Low Spin-Vibronic Energy Levels (cm$^{-1}$) of $CF_3O$ and $CF_3S$ Correlated to Asymmetric Normal Vibrations $Q_5$ and $Q_6$[a]**

| $\tilde{X}$ $^2$E $CF_3O$ | | | $\tilde{X}$ $^2$E $CF_3S$ | | |
|---|---|---|---|---|---|
| assignment | theory | exp[b] | assignment | theory | exp[b] |
| $0_0$(E), $j = 1/2$ | 0 ($E_{3/2}$) | 0 | $0_0^-$(E), $j = 1/2$ | 0 ($E_{3/2}$) | 0 |
| $0_0$(E*), $j = 1/2$ | 42 ($E_{1/2}$) | 41 | $0_0^+$(E*), $j = 1/2$ | 165 ($E_{1/2}$) | 159 |
| $6_1$($A_1$), $j = 3/2$ | 272 ($E_{1/2}$) | 249 | $6_1^-$($A_1$), $j = 3/2$ | 260 ($E_{1/2}$) | 248 |
| $6_1$($A_2$), $j = 3/2$ | 317 ($E_{1/2}$) | 306 | $6_1^+$($A_2$), $j = 3/2$ | 399 ($E_{1/2}$) | 387 |
| $6_1$(E), $j = 1/2$ | 536 ($E_{3/2}$) | 505 | $6_2^-$(E), $j = 1/2$ | 474 ($E_{3/2}$) | 463 |
| $6_1$(E*), $j = 1/2$ | 550 ($E_{1/2}$) | 526 | $6_2^-$(E), $j = 5/2$ | 523 ($E_{1/2}$) | |
| $6_2$(E), $j = 5/2$ | 592 ($E_{1/2}$) | | $5_1^-$(E), $j = 1/2$ | 557 ($E_{1/2}$) | 538 |
| $5_1$($A_1$), $j = 3/2$ | 601 ($E_{1/2}$) | 570 | $5_1^-$($A_1$), $j = 3/2$ | 564 ($E_{1/2}$) | |
| $6_2$(E*), $j = 5/2$ | 602 ($E_{3/2}$) | | $6_2^+$(E*), $j = 1/2$ | 589 ($E_{1/2}$) | 569 |
| $5_1$(E), $j = 1/2$ | 657 ($E_{1/2}$) | 631 | $6_2^+$(E*), $j = 5/2$ | 644 ($E_{3/2}$) | |
| $5_1$($A_2$), $j = 3/2$ | 675 ($E_{1/2}$) | 581 | $5_1^+$($A_2$), $j = 3/2$ | 727 ($E_{1/2}$) | |
| $5_1$(E*), $j = 1/2$ | 684 ($E_{3/2}$) | 656 | $5_1^+$(E*), $j = 1/2$ | 735 ($E_{3/2}$) | 715 |

[a] Spin-vibronic eigenstates were approximately correlated to the vibronic states of $A_1$, $A_2$, or E symmetry with the JT quantum number $j = |l \pm 1/2|$ where $l$ is the vibrational angular momentum quantum number corresponding to a $v$-quantum excitation of normal vibrations $Q_5$(E) and $Q_6$(E) ($5_v$ or $6_v$, respectively). The asterisk denotes another component of the E-symmetry level split by SOC. Spin-vibronic eigenstates of $CF_3S$ were also correlated to the upper (+) and lower (−) spin−orbit components of the $\tilde{X}$ $^2$E adiabatic electronic state. [b] Experiment: laser-induced dispersed fluorescence.[4,20]

Figure 2 illustrates the importance of spin-vibronic and multimode couplings[43] for an adequate description of a strongly nonadiabatic system using $\tilde{X}$ $^2$E $CF_3S$ as an example. Inclusion of JT coupling terms and SOC in the treatment complicates the spectroscopy of $CF_3S$, resulting in splitting and shifting the vibrational levels (cf. Figure 2a and Figure 2b,c) calculated even in the single mode approximation. Inclusion of all six vibrational modes in the treatment provides the full set of spin-vibronic levels that is as rule not just a superposition of different normal vibrations but also includes multimode coupling: cf. Figure 2c and Figure 2d. The significance of the latter was clarified by comparison of eigenenergies calculated within the single mode approach with the corresponding values calculated with inclusion of all vibrational modes. In the present study, we consider only the most significant vibronic coupling that is between the normal modes $Q_5$(E) and $Q_6$(E), the other multimode interactions are neglected for simplicity (they are actually small). Our previous studies[22,23] on $CH_3O$ and $CH_3S$ address the issue of multimode coupling (that is more significant for these species) in more detail.

Table 3 shows results of calculations of the low spin-vibronic energy levels in $\tilde{X}$ $^2$E $CF_3O$ and $CF_3S$ approximately assigned in terms of single normal oscillators corresponding to the most active JT modes: FCF-deformation $Q_5$(E) and FC$X$-deformation $Q_6$(E). The spin-vibronic states of $CF_3O$ with a moderate JT effect accompanied by a weak SOC can be interpreted as vibronic levels split or shifted by SOC. In the case of a strong SOC ($\tilde{X}$ $^2$E $CF_3S$), spin-vibronic levels can be correlated to one of the two spin−orbit states $E_{3/2}$ and $E_{1/2}$ arising from the electronic E-term split by SOC. The higher energy spin-vibronic states are more strongly mixed than the lower ones, and their assignments in terms of harmonic oscillators may be more difficult or meaningless. Note also that each of the spin-vibronic

**TABLE 4: Fundamental Energy Levels Assigned to $Q_1(A_1)$, $Q_2(A_1)$, $Q_3(A_1)$, and $Q_4(E)$[a]**

| | $\tilde{X}\ ^2E$ $CF_3O$ | | $\tilde{X}\ ^2E$ $CF_3S$ | |
|---|---|---|---|---|
| assignment | theory | exp | theory | exp[b] |
| $1_1^-(E)$ | 1335 ($E_{3/2}$) | 1216,[b] 1273,[c] 1260 [d] | 795 ($E_{3/2}$) | 767 |
| $1_1^+(E^*)$ | 1377 ($E_{1/2}$) | 1240 [b] | 960 ($E_{1/2}$) | 924 |
| $2_1^-(E)$ | 937 ($E_{3/2}$) | 977,[b] 891,[c] 894 [d] | 1191 ($E_{3/2}$) | 1131 |
| $2_1^+(E^*)$ | 979 ($E_{1/2}$) | 1002 [b] | 1356 ($E_{1/2}$) | 1291 |
| $3_1^-(E)$ | 648 ($E_{3/2}$) | 527,[b] 621,[c] 622 [d] | 468 ($E_{3/2}$) | 444 |
| $3_1^+(E^*)$ | 690 ($E_{1/2}$) | 550 [b] | 634 ($E_{1/2}$) | 614 |
| $4_1^-(A_1)$ | 1316 ($E_{1/2}$) | 1215−1207,[c] 1199−1207 [d] | 1263 ($E_{1/2}$) | |
| $4_1^-(E)$ | 1329 ($E_{1/2}$) | | 1264 ($E_{1/2}$) | |
| $4_1^+(E^*)$ | 1369 ($E_{3/2}$) | | 1428 ($E_{3/2}$) | |
| $4_1^+(A_2)$ | 1384 ($E_{1/2}$) | | 1430 ($E_{1/2}$) | |

[a] These eigenstates were approximately correlated to the vibronic states of $A_1$, $A_2$, or E symmetry corresponding to a $v$-quantum excitation of normal vibrations $Q_1(A_1)$, $Q_2(A_1)$, $Q_3(A_1)$, and $Q_4(E)$ and to the upper (+) and lower (−) spin−orbit components of the $\tilde{X}\ ^2E$ adiabatic electronic state. The asterisk denotes another component of the E-symmetry level split by SOC. [b] Laser-induced dispersed fluorescence, gas.[4,20] [c] Infrared spectrum, neon matrix.[45] [d] Infrared spectrum, argon matrix.[45]

levels in Table 3 classified according to irreducible presentations ($E_{1/2}$, $E_{3/2}$) of the double $C_{3v}$ symmetry group is still 2-fold degenerate with respect to the electronic spin vector; this is the Kramers degeneracy of systems with an odd number of fermions that can be lifted by an external field breaking down the time-reversal symmetry of the total Hamiltonian (for instance, in an external magnetic field).

Table 4 presents fundamental wavenumbers assigned to normal vibrations $Q_1(A_1)$, $Q_2(A_1)$, $Q_3(A_1)$, and $Q_4(E)$. Each of the $1_1$, $2_1$, $3_1$, and $4_1$ vibrational levels undergoes the spin−orbit splitting of about 42 ($CF_3O$) and 165 ($CF_3S$) $cm^{-1}$. The $4_1$ vibrational state corresponding to an asymmetric normal mode is split due to the Jahn−Teller effect; the vibronic splitting of $4_1$ is larger in $\tilde{X}\ ^2E$ $CF_3O$ than in $\tilde{X}\ ^2E$ $CF_3S$, whereas the spin−orbit splitting in $\tilde{X}\ ^2E$ $CF_3S$ is much more noticeable.

In conclusion, we make a comparison of calculated wavenumbers with available experimental data. Table 3 shows the intervals obtained from the laser-induced dispersed fluorescence spectra[4,20] of the $CF_3O$ and $CF_3S$ radicals and assigned to the FCF- and FC*X* deformations that generate the most pronounced net JT effects in $\tilde{X}\ ^2E$ $CF_3O$ and $CF_3S$. The theoretical value of spin−orbit splitting in the ground vibronic state of $CF_3O$ ($a\zeta_e d = 42$ $cm^{-1}$) and $CF_3S$ ($a\zeta_e d = 165$ $cm^{-1}$) is very close to the observed ones. The Ham reduction factor $d$ ($d \leq 1$) in $a\zeta_e d$ (Tables 2 and 3) indicates how much the spin−orbit coupling ($a\zeta_e$) is reduced by the Jahn−Teller effect.[4,20] Although the discrepancy becomes larger for higher energy spin-vibronic levels, the agreement between theory and experiment remains good enough to demonstrate the robustness of the model described in this paper despite the approximations used. Theory can also supply the missing experimental wavenumbers that could not be resolved in the dispersed fluorescence spectrum: for instance, the eigenstates assigned to $j_{JT} = \pm 5/2$ (Table 3) are unlikely to be observed due to the low (zero) intensity expected for the corresponding transitions.[4,20] Besides, no experimental intervals were identified for the asymmetric C−F stretching in $\tilde{X}\ ^2E$ $CF_3S$.[20,44−47] In regard to other wavenumbers given in Table 4, discrepancies between theory and experiment are larger than those in Table 3, in particular, with respect to the C−F stretching in $\tilde{X}\ ^2E$ $CF_3O$. However, the deviation between theory and experiment is quite understandable, taking into account the fact that some of the intervals in Table 4 were observed for matrix-isolated radicals,[45−47] spectra of which can be significantly different from those of the gas-phase species we calculate. On the other hand, the experimental data[20,44−47] are in disagreement between themselves for some of these wavenumbers (see Table 4).

## Conclusions

This paper reports results of an ab initio study of the nonadiabatic (spin-vibronic) dynamics in the ground electronic state $\tilde{X}\ ^2E$ of $CF_3O$ and $CF_3S$, the fluorinated analogs of the methoxy radical $CH_3O$. These radicals are subject to the Jahn−Teller effect breaking down the Born−Oppenheimer adiabatic approximation by splitting the degenerate electronic state along the asymmetric vibrational modes, and making a solution of the nuclear Schrödinger equation within a single adiabatic energy surface meaningless.

We have performed a variational solution of the nuclear dynamics problem for two strongly coupled electronic states correlating to the 2-fold degenerate electronic state $\tilde{X}\ ^2E$ of $CF_3O$ and $CF_3S$. The interplay of Jahn−Teller and spin−orbit couplings in these species gives rise to spin-vibronic interactions. Neither of these effects has been neglected; they both have been treated on an equal footing by means of simultaneous inclusion of the corresponding parameters in the model Hamiltonian. The multimode E⊗E eigenproblem has been solved including higher order Jahn−Teller and anharmonic terms which are found to be important in description of the Jahn−Teller potential energy surfaces in the vicinity of the conical intersection as well as in the area of the global minimum corresponding to the Jahn−Teller distorted nuclear configuration; thereby, these terms are critically important for the high precision evaluation of spin-vibronic energy levels of $CF_3O$ and $CF_3S$. The agreement between theoretically predicted and experimentally observed wavenumbers has been found to vary from fair to impressive without any adjustment of the model parameters to the corresponding experimental data.

**Acknowledgments** are made to the Donors of the ACS Petroleum Research Fund and to the Welch Foundation (grant F-100) for support of this research. We thank Terry Miller and Donald Truhlar for illuminating discussions of these studies, and we are also grateful to John Stanton for the opportunity to use his expanded version of the ACES II program. The study is part of the work of the IUPAC working party on the thermodynamics of atmospheric free radicals.

## References and Notes

(1) Born, M.; Oppenheimer, R. *Ann. Phys.* **1927**, *84*, 457.
(2) *Conical Intersections: Electronic Structure, Dynamics & Spectroscopy*; Domcke, W., Yarkony, D. R., Köppel, H., Eds.; World Scientific: River Edge, NJ, 2004.
(3) Schreiber, E. *Femtosecond Real-Time Spectroscopy of Small Molecules and Clusters*; Springer: New York, 1998.
(4) Barckholtz, T. A.; Miller, T. A. *Int. Rev. Phys. Chem.* **1998**, *17*, 435.
(5) *Applied Laser Spectroscopy: Techniques, Instrumentation, and Applications*; Andrews, D. L., Ed.; VCH: New York, 1992.
(6) In *Molecular Dynamics and Spectroscopy by Stimulated Emission Pumping*; Dai, H.-L., Field, R. W., Eds.; World Scientific: Singapore, 1995.
(7) Baer, M. *Beyond Born-Oppenheimer: Electronic Nonadiabatic Coupling Terms and Conical Intersections*; Wiley-Interscience: Hoboken, NJ, 2006.
(8) Mead, C. A.; Truhlar, D. G. *J. Chem. Phys.* **1982**, *77*, 6090.
(9) Berry, M. V. *Proc. R. Soc. London A* **1984**, *392*, 45.
(10) Mead, C. A.; Truhlar, D. G. *J. Chem. Phys.* **1979**, *70*, 2284.
(11) Mead, C. A. *Rev. Mod. Phys.* **1992**, *64*, 51.
(12) Garcia-Fernandez, P.; Bersuker, I. B.; Boggs, J. E. *Phys. Rev. Lett.* **2006**, *96*, 163005−1.
(13) Yarkony, D. R. *J. Phys. Chem. A* **2001**, *105*, 6277.
(14) Jahn, H. A.; Teller, E. *Proc. R. Soc., London A* **1937**, *161*, 220.

(15) Englman, R. *The Jahn-Teller Effect in Molecules and Crystals*; Wiley-Interscience: New York, 1972.
(16) Bersuker, I. B. *The Jahn-Teller Effect*; Cambridge University Press: Cambridge, U.K., 2006.
(17) Viel, A.; Eisfeld, W. *J. Chem. Phys.* **2004**, *120*, 4603.
(18) Garcia-Fernandez, P.; Bersuker, I. B.; Aramburu, J. A.; Barriuso, M. T.; Moreno, M. *Phys. Rev. B* **2005**, *71*, 184117−1.
(19) Ham, F. S. *Phys. Rev.* **1965**, *138*, 1727.
(20) Barckholtz, T. A.; Yang, M.-C.; Miller, T. A. *Mol. Phys.* **1999**, *97*, 239.
(21) Marenich, A. V.; Boggs, J. E. *Int. J. Quantum Chem.* **2006**, *106*, 2609.
(22) Marenich, A. V.; Boggs, J. E. *J. Chem. Phys.* **2005**, *122*, 024308−1.
(23) Marenich, A. V.; Boggs, J. E. *J. Chem. Theory Comput.* **2005**, *1*, 1162.
(24) Wigner, E. P. *Group Theory and its Application to the Quantum Mechanics of Atomic Spectra*; Academic Press: New York, 1959.
(25) Mead, C. A. *J. Chem. Phys.* **1979**, *70*, 2276.
(26) Koizumi, H.; Sugano, S. *J. Chem. Phys.* **1995**, *102*, 4472.
(27) Schön, J.; Köppel, H. *J. Chem. Phys.* **1998**, *108*, 1503.
(28) Hougen, J. T. *J. Mol. Spectrosc.* **1980**, *81*, 73.
(29) Bunker, P. R.; Jensen, P. *Molecular Symmetry and Spectroscopy*, 2nd ed.; NRC Research: Ottawa, Canada, 1998.
(30) Flurry, R. L., Jr. *Symmetry Groups: Theory and Chemical Applications*; Prentice Hall: Englewood Cliffs, NJ, 1980.
(31) Domcke, W.; Mishra, S.; Poluyanov, L. V. *Chem. Phys.* **2006**, *322*, 405.
(32) Sliznev, V. V. Private communication. Solomonik, V. G. Doctor in Chemistry Thesis, Moscow State University, 1993.
(33) Stanton, J. F.; Gauss, J.; Watts, J. D.; Lauderdale, W. J.; Bartlett, R. J. *Int. J. Quantum Chem.: Quantum Chem. Symp.* **1992**, *26*, 879.
(34) Stanton, J. F.; Bartlett, R. J. *J. Chem. Phys.* **1993**, *98*, 7029.
(35) Stanton, J. F.; Gauss, J. *J. Chem. Phys.* **1994**, *101*, 8938.
(36) Dunning, T. H., Jr. *J. Chem. Phys.* **1989**, *90*, 1007.
(37) Peterson, K. A.; Dunning, T. H., Jr. *J. Chem. Phys.* **2002**, *117*, 10548.
(38) Basis sets were obtained from the Extensible Computational Chemistry Environment Basis Set Database, Version 02/25/04, as developed and distributed by the Molecular Science Computing Facility, Environmental and Molecular Sciences Laboratory which is part of the Pacific Northwest Laboratory, P.O. Box 999, Richland, WA 99352, U.S.A., and funded by the U.S. Department of Energy. The Pacific Northwest Laboratory is a multiprogram laboratory operated by Battelle Memorial Institute for the U.S. Department of Energy under contract DE-AC06-76RLO 1830. Contact Karen Schuchardt for further information.
(39) Schmidt, M. W.; Baldridge, K. K.; Boatz, J. A.; Elbert, S. T.; Gordon, M. S.; Jensen, J. H.; Koseki, S.; Matsunaga, N.; Nguyen, K. A.; Su, S.; Windus, T. L.; Dupuis, M.; Montgomery, J. A., Jr. *J. Comput. Chem.* **1993**, *14*, 1347.
(40) Fedorov, D. G.; Koseki, S.; Schmidt, M. W.; Gordon, M. S. *Int. Rev. Phys. Chem.* **2003**, *22*, 551.
(41) Nakano, H. *J. Chem. Phys.* **1993**, *99*, 7983.
(42) Nakajima, T.; Hirao, K. *Chem. Phys. Lett.* **1999**, *302*, 383.
(43) Köppel, H.; Domcke, W.; Cederbaum, L. S. *Adv. Chem. Phys.* **1984**, *57*, 59.
(44) Jacox, M. E. *J. Phys. Chem. Ref. Data* **2003**, *32*, 1.
(45) Argüello, G. A.; Willner, H. *J. Phys. Chem. A* **2001**, *105*, 3466.
(46) Andrews, L.; Hawkins, M.; Withnall, R. *Inorg. Chem.* **1985**, *24*, 4234.
(47) Clemitshaw, K. C.; Sodeau, J. R. *J. Phys. Chem.* **1989**, *93*, 3552.